

Nature and strength of bonding in a crystal of semiconducting nanotubes: van der Waals density functional calculations and analytical results

Jesper Kleis,^{1,2} Elsebeth Schröder,¹ and Per Hyldgaard^{3,*}

¹*Department of Applied Physics, Chalmers University of Technology, SE-412 96 Göteborg, Sweden*

²*CAMD, Department of Physics, Technical University of Denmark, DK-2800 Kgs. Lyngby, Denmark*

³*Department of Microtechnology and Nanoscience, MC2, Chalmers University of Technology, SE-412 96 Göteborg, Sweden*

(Dated: November 20, 2021)

The dispersive interaction between nanotubes is investigated through ab initio theory calculations and in an analytical approximation. A van der Waals density functional (vdW-DF) [Phys. Rev. Lett. **92**, 246401 (2004)] is used to determine and compare the binding of a pair of nanotubes as well as in a nanotube crystal. To analyze the interaction and determine the importance of morphology, we furthermore compare results of our ab initio calculations with a simple analytical result that we obtain for a pair of well-separated nanotubes. In contrast to traditional density functional theory calculations, the vdW-DF study predicts an intertube vdW bonding with a strength that is consistent with recent observations for the interlayer binding in graphitics. It also produce a nanotube wall-to-wall separation which is in very good agreement with experiments. Moreover, we find that the vdW-DF result for the nanotube-crystal binding energy can be approximated by a sum of nanotube-pair interactions when these are calculated in vdW-DF. This observation suggests a framework for an efficient implementation of quantum-physical modeling of the CNT bundling in more general nanotube bundles, including nanotube yarn and rope structures.

PACS numbers: 61.50.Lt, 61.46.-w, 71.15.Mb

I. INTRODUCTION

Carbon nanotubes (CNTs) have a wealth of exciting physical properties that have made them the focus for a very broad range of fundamental-science studies.¹ The CNTs have, for example, an exceptionally large Young's modulus.² The individual CNTs have nanoscale diameters and micronscale lengths but a range of CNT assembly processes promise technology applications even on more macroscopic scales. Thermal treatment can cause a fullerene source to transform into a highly regular CNT crystal with parallel tubes aligned in a hexagonal structure.³ The tubes can also form CNT bundles^{4,5,6,7} in which essentially parallel CNTs still have a very high degree of (local) order. The bundles can be spun into yarn^{8,9} and further twisted to produce torque-free ropes of micrometer diameter (and arbitrary length). The yarn and ropes have a large strength and a unique ability to absorb elastic energy in reversible extensions.⁹ By pre-selecting the nanotube source material, for example, as single-walled CNTs,¹⁰ it is possible to ensure specific physical properties (like metallic conductivity) also of the resulting well-aligned yarn.^{9,11}

The science^{1,2,3,4,5,6,7} and technology progress^{8,9,10,11} challenges us to present a quantum-physical characterization of the bonding in the nanotube crystal³ and, by extension, in the bundles. It is valuable to have a method for parameter-free characterization of general CNT bundles and it is important to test the accuracy of available computational tools. The CNT crystals (and bundles) are (approximately) periodic and have a relatively simple order. This makes them accessible to calculations in density functional theory (DFT) which, in principle, provides quantum-physical accounts of general mate-

rial bonding. It is straightforward to provide quantum-physical calculations for a parameter-free characterization of the intra-CNT electronic and atomic organization using traditional implementations of state-of-the-art DFT calculations.^{12,13} These calculations use either the local density approximation (LDA)¹⁴ and/or the semilocal generalized gradient approximation (GGA), for example, as parameterized in the Perdew-Burke-Ernzerhof flavor.¹⁵ However, the CNT crystals and bundles are graphitic materials and the intertube attraction is known to be dominated by relatively soft dispersive or van der Waals (vdW) interactions.^{3,16} Neither LDA nor GGA provide any physics-based account of the bonding between the CNTs.^{17,18,19,20,21}

In this paper we use a recently developed van der Waals density functional^{22,23} (vdW-DF) to provide a quantum physical account of the vdW bonding in a hexagonal crystal³ of parallel semiconducting nanotubes. We perform state-of-the-art DFT calculations of the intra-nanotube structure within GGA and of the inter-nanotube binding within vdW-DF. The study testifies to the strength of this vdW bonding, which is normally described as soft but nevertheless contributes significantly to the cohesion of the CNT crystal. Our results allow a test of the vdW-DF theory method by comparison against structure measurements for the highly ordered CNT crystal³ and bundle⁶ structures. The study supplements a recent vdW-DF calculation²⁴ on a simple polymer, polyethylen, for which there also exists experimental characterization of the crystalline structure.²⁵ It also supplements vdW-DF calculations of the benzene and DNA base-pair interactions²⁶ in a wider program on calculating dispersive interactions in carbon and organic materials. We provide a parameter-free theory determi-

nation of the CNT bonding in the crystal and between pairs of parallel nanotubes and document that a summation of nanotube-pair interaction energies (calculated in vdW-DF) represents a fair approximation for the vdW-DF results for the crystal bundling energy. We also detail the nature of the mutual CNT interactions by identifying a set of distinct vdW interaction regimes. We show that the vdW interaction is significantly enhanced at the bonding separation compared with the value estimated from the asymptotic interaction.

The vdW-DF calculations correct the accuracy problems arising in traditional state-of-the-art implementations of DFT (that uses LDA or GGA) without loss of the traditional-DFT scaling²³ (computation cost increasing $\sim \mathcal{O}(N^3)$ with system size). DFT calculations in GGA show no meaningful binding.²⁷ While LDA calculations can mimic the CNT binding it underestimates the binding separation. For the CNT bundles, the LDA result²⁸ for the wall-to-wall separation, $\Delta_{\text{LDA}} = 3.1 \text{ \AA}$, is 10% shorter than the experimental value, $\Delta_{\text{CNT}} = 3.4 \text{ \AA}$. Moreover, the LDA result,²⁸ $\approx 10 \text{ meV/atom}$, for the intertube binding in a crystal of metallic (6,6) CNTs is significantly smaller than the estimate²⁹ (50 meV/atom for graphitics materials) extracted from measurements of the binding of polyaromatic hydrocarbon (PAH) molecules on graphite. The vdW-DF method corrects those problems without loss of scaling advantages by supplementing the LDA for correlation with a nonlocal contribution²² that scales like $\mathcal{O}(N^2)$ with the system size.²³ The vdW-DF method clearly has a better scaling than implementations of canonical Møller-Plesset perturbation theory (MP2) for extended structures like polymer crystals.³⁰ Specially adapted MP2 implementations can achieve a linear scaling with size for large molecules.³¹ The adapted MP2 method has also been applied to extended one-dimensional systems.³² It is unclear how the adapted-MP2 evaluation of correlation and the vdW-DF determination of nonlocal correlation compare in actual computing cost for extended structures like polymer crystals^{24,32} and for large bulk and surface-adhesion systems.^{21,33,34,35} In any case, the complete MP2 calculation³² also involves Hartree-Fock calculations which scale worse than general DFT implementations (including, for example, vdW-DF).

The paper is organized as follows. In section II we identify regimes of interactions in crystals of nanotubes and discuss qualitative differences in the vdW bonding of semiconducting and of metallic nanotubes. Section III presents a summary of the vdW-DF calculation method that we use to obtain an ab initio characterization of the semiconducting-nanotube crystal. In section IV we present an analytical description of the nanotube interaction and in section V we discuss both the strength and nature of the inter-nanotube interaction. Section VI contains our conclusions and acknowledgements.

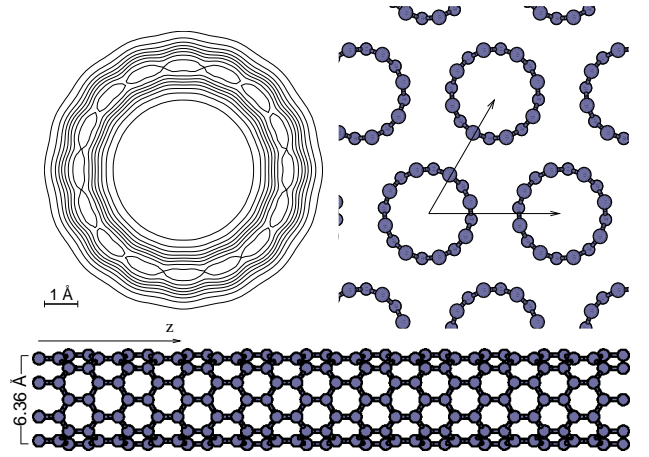


FIG. 1: Atomic and electronic structure as well as filament organization in crystals of semiconducting (8,0) zigzag nanotubes. *The lower panel* shows the fully relaxed atomic configuration of the individual (8,0) nanotubes as calculated in a traditional implementation of ab initio density functional theory (DFT). *The top left panel* shows our corresponding traditional DFT results for the length-averaged electron density concentrated at the atomic nuclei; the contour spacing is specified in steps of 0.15 e\AA^3 . Finally, *the top right panel* shows the hexagonal crystalline order of the nanotube bundle. We calculate the intertube dispersive interaction and determine the nanotube crystalline structure using a recently developed ab initio van der Waals density functional approach.²²

II. REGIMES OF NANOTUBE INTERACTIONS

There are several regimes of interactions relevant for the cohesion of the nanotube crystals. The individual tubes are held together by exceptionally strong covalent bonds between neighboring carbon atoms separated by just 1.42 \AA . The binding *between* the CNTs is instead dominated by the vdW interaction that binds the tubes at a wall-to-wall CNT separation of 3.4 \AA . The vdW interaction also causes an inter-tube attraction even at asymptotic distances. There are qualitative differences in the vdW forces in the asymptotic regime (where the interaction is defined by the dipolar electro-dynamical response) and at bonding separation in graphitics materials (where multipolar contributions are documented to enhance the interaction.)²⁰

Moreover, the vdW interaction between extended semiconducting and metallic structures (for example, semiconducting and metallic CNTs) is qualitatively different, at least in the regime of asymptotic interactions.^{23,36,37,38,39} Single-walled CNTs can exhibit both a semiconducting and metallic nature of conduction depending on their chirality. Being low-dimensional systems, the semiconducting and metallic CNTs therefore exhibit significant differences in their electronic response and, consequently, in the asymptotic vdW interactions.^{36,37,38,39} In the strictly asymptotic regime it is possible to view the CNT as wires. For a pair of insulat-

ing or semiconducting wires, the asymptotic form of the interaction is known to *eventually* acquire a d^{-5} dependence with the separation d between the wire centers of mass. In contrast, Dobson *et al.* recently used a coupled-plasmon expansion and approximations valid for asymptotic mutual separations to derive a mutual interaction energy with a $-d^{-2}(\log(d))^{-3/2}$ asymptotic scaling for metallic wires.³⁹ It is not known to what extent qualitative differences between the vdW binding of metallic and semiconducting nanotubes persist down to distances relevant for their binding in CNT pairs or bundles²³ but that is an important question beyond the present scope. Extraction of CNT binding energies from the metallic-wire study Ref. 39 is complicated because there are two convoluted interaction effects arising as the CNTs approach each other. Firstly, the CNT morphology (a hollow cylinder) manifests itself^{40,41} even when the long-wavelength form of the mutual dielectric response remains applicable. Secondly, the nature of the van der Waals interaction changes²⁰ so that it is no longer dominated by the long-wavelength response form, but also retains interaction contributions defined by the multipole response.²⁰

Figure 1 shows schematics of the electronic, (intra-tube) atomic, as well as (inter-tube) crystalline ordering (bundling) of nanotubes. We study the mutual binding of pairs and bundles of CNTs that have a chirality vector¹ (8,0). These CNTs have a diameter a little larger than 0.6 nm, a four-fold rotational symmetry, and an along-axis structure repeating itself every 32 atoms. Confirming also previous investigations,¹³ we find that state-of-the-art DFT calculations using GGA provide an excellent account of the intra-nanotube structural organization and electronic properties such as the nature of conduction. We use the traditional DFT-GGA results, obtained in a plane-wave implementation,⁴² as the starting point for vdW-DF calculations of the intertube binding.^{22,23}

Recent density-functional approximations by us^{20,22,23,43,44} and by others^{45,46,47,48,49} extend traditional DFT to provide a seamless, parameter-free characterization of the vdW binding without introducing double counting at separations with finite overlap of electron densities. In our vdW-DF method^{22,23} we extract the exchange from GGA calculations but supplement the local density approximation for the correlation energy by a nonlocal correlation energy contribution E_c^{nl} . This contribution is evaluated from the electron densities of the underlying traditional DFT calculations in GGA. This vdW-DF description remains applicable and effective even for large extended systems that are accessible for standard ab initio DFT calculation (although at an increase in computing cost). In fact, the vdW-DF method exhibits the same scaling as the underlying traditional DFT calculations.²³ The vdW-DF approach permits ab initio characterizations of large bulk systems, for example, produced by potassium intercalation.²¹ It further permits *ab initio* investigations of very large surface-adhesion systems, for example, graphite-adsorption of PAH molecules.^{33,34} In a con-

trolled approximation it even permits an ab initio study (in a repeated unit cell containing 146 atoms) of the adhesion of graphite sheets on SiC surfaces.³⁵

The vdW-DF evaluation of the nonlocal correlations E_c^{nl} (vdW interaction energy) involves a density-weighted integration of a kernel²² that contains a rich account of the complex electrodynamics.^{20,22,23,44} Our vdW-DF is not developed to include an explicit account of the asymptotic interaction between extended metallic one-dimensional systems.²³ The form of the vdW-DF kernel^{22,23} ensures the correct asymptotic behavior of vdW interactions for atoms, molecules, and most surface and bulk systems. It also describes the asymptotic interactions for extended low-dimensional systems that are isolating or semiconducting. The form of the vdW-DF kernel ensures the correct asymptotic form of the interaction between pairs and within crystals of the (8,0) CNTs because these are robustly semiconducting (characterized by a significant gap¹). More importantly, our vdW-DF calculations of the (8,0)-CNT binding not only *eventually* reproduces a d^{-5} dependence in the interaction energies but reveals a much finer structure and remains fully applicable at general separations.

To interpret this rich structure in CNT binding-energy variation with CNT separation, we also present in this paper an analytical evaluation of the CNT-pair interaction, valid at intermediate-to-asymptotic distances. Our analysis tool (but not our full vdW-DF calculations) makes assumptions of non-overlapping electron densities and of a long-wavelength form of the CNT dielectric response but it respects the CNT morphology.^{41,50,51} Comparison with the full vdW-DF calculations therefore allows us to deconvolute effects arising from the change in nature of the dielectric response. We thereby provide an analysis that splits the interaction into two major regimes: (1) a close regime at or near binding separations where full ab initio vdW-DF calculations are essential for an accurate account and (2) an intermediate-to-asymptotic regime where the long-wavelength dielectric response remains applicable but where the CNT morphology specifies the variation of the interaction. The result of this analysis documents that the vdW interaction enhances at bonding separations compared with estimates that can be extracted from knowledge of the asymptotic form of the inter-nanotube bonding.

III. COMPUTATIONAL METHODS

The top right panel of Fig. 1 shows a schematic of the repeated two-dimensional hexagonal array of the nanotube bundles. We apply the vdW-DF²² method to include the dispersive interaction within the framework of traditional plane-wave DFT both for dimers of nanotubes as well as for an infinitely extended nanotube crystal (Figure 1). A self-consistent formulation of vdW-DF has recently been derived, implemented, and tested.²³ Here we use the original, non-selfconsistent (post-GGA) imple-

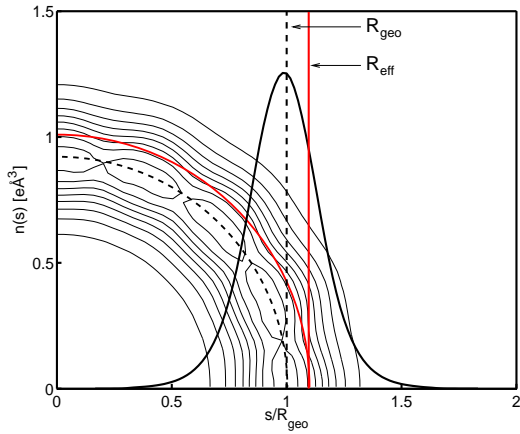


FIG. 2: Length- and radially-averaged electron density $\bar{n}(s)$ shown together with the positions of the effective and the geometric radius. The radial separation is given relative to the geometric radius of the nanotube. The background inset shows the length averaged electron density with contour lines separated in steps of $0.15 \text{ e}\text{\AA}^3$.

mentation²² that rests upon and utilizes traditional DFT calculations to obtain the electron density variations.

In the present vdW-DF study we furthermore take advantage of the success of the traditional semi-local (GGA) density functionals to describe the *intra*-molecular properties of the nanotubes (as well as the electron densities). It is, in principle, possible to provide an all-vdW-DF characterization of the intra-nanotube atomic structure (allowing relaxation under vdW-DF forces²³) but the computation costs would be large. Our previous experience from an all-vdW-DF characterization of a single graphite sheet²¹ suggests that only minute differences would result for the CNT structure if we replaced the GGA intra-tube characterization by a full vdW-DF characterization.

A. Nanotube atomic and electronic structure

In the actual vdW-DF implementation, a large set of state-of-the-art traditional DFT calculations determine the atomic structure (of the individual nanotube) and the electron density variation of the nanotubes when isolated, when assembled into a hexagonal crystalline structure, or when aligned as a parallel nanotube dimer. We use a plane-wave code⁴² with ultra-soft pseudopotentials and a $1 \times 1 \times 8$ Monkhorst-Pack⁵² k -point sampling of the Brillouin zone of the periodically repeated unit cell containing 32 atoms per nanotube. We perform self-consistent calculations in the Perdew-Burke-Ernzerhof (PBE)-flavor¹⁵ of GGA for the exchange and correlation functional. We choose a plane-wave energy cut-off 476 eV and specify the Fast Fourier Transform (FFT) grid so that the (density) grid spacing remains smaller than 0.14

\AA in all directions.

We first determine the atomic structure of the individual (8,0) nanotube, lower panel of Fig. 1. We use our ab initio calculations of the strong intra-nanotube atomic forces to relax the morphology to a total residual atomic force $0.05 \text{ eV}/\text{\AA}$ per unit cell. The structure is characterized by an effective geometrical radius R_{geo} specified as the average distance of the carbon nuclei from the axis defined by the nanotube center of mass. We determine the value of that geometric radius to be $R_{\text{geo}} = 3.18 \text{ \AA}$. As explained above, the atomic structure (obtained in PBE-GGA for the isolated nanotube) is kept frozen in all subsequent calculations (for nanotube crystal and dimer cases). We have explicitly tested that no additional intratube atomic-relaxation is relevant at (or beyond) the separation that characterizes the nanotube-crystal/dimer binding in our subsequent post-GGA vdW-DF characterization.

Next we determine the electronic structure from traditional DFT calculations for the isolated nanotubes, for the nanotube bundles, and for the dimer structures. The upper left panel of Fig. 1 shows contours (at $0.15 \text{ e}\text{\AA}^{-3}$ interval) in the isolated-nanotube electron density variation averaged along the nanotube axis. The maximum in electron density coincides with the radial position of nuclei and naturally identifies the nanotube wall. To characterize the inter-nanotube vdW-dominated binding we further calculate the electron density for nanotubes in hexagonal crystals and dimers as a function of the wall-to-wall nanotube separation Δ and as a function of the nanotube rotation angle (relative rotation angle in the case of the dimer study).

We find that there are important electron-density overlaps for $\Delta < 4 \text{ \AA}$ when the self-consistent GGA electron densities differ from a superposition of individual-nanotube electron densities. The existence of these intertube electron-density overlaps has direct consequences for the details of the intertube vdW binding. However, the electron-density overlap does not reflect the existence of any relevant (and physically meaningful) binding arising within the GGA calculations themselves (in any of the GGA flavors).

B. van der Waals density functional theory

Like the LDA and GGA functionals, the vdW-DF is defined by approximations for the exchange and correlation energies. The nonlocal dispersive interactions responsible for keeping the bundle of nanotubes together are included as a significant extension (correction) of the correlations energy in the underlying GGA calculations. Specifically, we completely replace the GGA description of correlation but use the self-consistent GGA result for the electron density to evaluate a new correlation energy that includes the nonlocal nature of the vdW binding.

Our vdW-DF splits the correlation up into local and

nonlocal contributions:^{22,43}

$$E_c \approx E_c^{\text{LDA}} + E_c^{\text{nl}}, \quad (1)$$

with the local part approximated in the LDA. The nonlocal correlation energy is expressed^{22,43}

$$E_c^{\text{nl}} = \int_0^\infty \frac{du}{2\pi} \text{tr}[\ln(1 - V\tilde{\chi}) - \ln(\epsilon)] \quad (2)$$

where u is the imaginary frequency, V is the inter-electron Coulomb interaction potential, $\tilde{\chi}$ is the local-field density response. The isotropic dielectric function, $\epsilon = \text{tr}(1 + 4\pi\alpha)/3$, is also specified by the local-field density response, $\tilde{\chi} = \nabla \cdot \alpha \cdot \nabla$. The nonlocal correlation energy is further approximated

$$E_c^{\text{nl}}[n] = \frac{1}{2} \int d\mathbf{r} d\mathbf{r}' n(\mathbf{r}) \phi(\mathbf{r}, \mathbf{r}') n(\mathbf{r}'), \quad (3)$$

through a kernel ϕ specified by a number of sum rules²² and physics results.^{22,23,53} The interaction energy (3) is consistently constructed to vanish for a homogeneous system. The kernel ϕ is specified by a pair of local parameters $q_0(\mathbf{r})$ and $q_0(\mathbf{r}')$ that depend on the electron density and the density gradient. The kernel can be tabulated in advance in terms of an effective separation $D = [(q_0 + q_0')/2]|\mathbf{r} - \mathbf{r}'|$ and an asymmetry parameter $\delta = (q_0 - q_0')/(q_0 + q_0')$. The value of the q_0 's are chosen to reproduce the (plasmon-pole) response of a weakly perturbed electron gas, Ref. 22.

With the evaluation of the nonlocal energy contribution (from underlying GGA calculations of the electron densities) we arrive at a vdW-DF total energy calculation:⁴⁴

$$E^{\text{vdW-DF}} = E^0 + E_c^{\text{nl}}, \quad (4)$$

$$E^0 = E^{\text{GGA}} - E_c^{\text{GGA}} + E_c^{\text{LDA}}. \quad (5)$$

The GGA energy term E^{GGA} is here evaluated in the revPBE⁵⁴ flavor (based on the self-consistent calculations for the electron density that we obtain in the PBE flavor of GGA). Effectively this amounts to a small adjustment of the exchange contribution, which we do to minimize any potential artificial exchange binding in the plane-wave formalism used.^{20,22,44,55} The new (semilocal) energy contribution E^0 represents a modification of GGA that, for example, retains a description of the kinetic-energy repulsion as well as, for example, covalent³⁴ or ionic²¹ interactions.

C. van der Waals density functional calculations

The evaluation of the nonlocal correlation E_c^{nl} requires extra care due to a grid sensitivity of the functional form (3). The vdW binding in the nanotube crystal and dimer cases arises almost exclusively from a difference in nonlocal-correlation energy E_c^{nl} for the crystalline/dimer-structure and for the isolated nanotubes. However, the

intramolecular density variation causes a very large contribution to E_c^{nl} that must be carefully subtracted in our ab initio calculations of the inter-nanotube interaction. Moreover, the evaluation of this intra-nanotube E_c^{nl} energy is somewhat sensitive to the relative position of atomic positions and FFT grid points.²¹ Nevertheless, robust and efficient evaluation of the inter-nanotube binding is possible by simply ensuring that we calculate and subtract E_c^{nl} contributions for the isolated nanotube using FFT grid points that closely match those of the composite system, as further explained in Ref. 21.

In practice we evaluate the vdW-DF binding in the nanotube crystals and dimers by supplementing every interacting nanotube system by a suitable reference calculation of the isolated nanotube. We determine the binding in nanotube bundles by adding (at every nanotube separation) a DFT calculation of the electron density for a corresponding isolated nanotube located in a cell of double size in each of the two perpendicular directions and on a FFT grid that retains the absolute grid-point spacing.²¹ In our calculations of E_c^{nl} , for the underlying GGA calculation we use a FFT-grid spacing that is always smaller than 0.14 Å in any direction; this choice is found sufficient given our work to carefully synchronize the FFT gridding when we calculate the electron density for the interacting and isolated nanotube system.

The real-space implementation of E_c^{nl} is simply applied to extended systems as graphite²¹ and polyethylene²⁴ by evaluating E_c^{nl} for the unit cell electron density as well as the nonlocal interaction from its surrounding images. To accelerate the vdW-DF characterization we limit the evaluation of the multidimensional integral (3) to contributions from grid points having a density larger than 10^{-4} a.u. The use of such a density cut-off is strongly motivated by the excellent convergence that we have previously documented for graphitic systems even when a significant ionic bond supplements the binding from nonlocal correlations.²¹ The nonlocal correction from the surrounding electron density converges rapidly in terms of the separation to the unit cell. We have tested that it is in general sufficient to only include the interaction from the electron density that is less than 12 Å away from the unit-cell boundaries in the direction along the nanotube and 15 Å in the directions perpendicular to the nanotube axis. Nevertheless, to converge the E_c^{nl} calculations to a sub-meV level and retain a very high relative accuracy even in the asymptotic regime, we choose to retain E_c^{nl} -contributions originating from points closer than 24 Å (and in some cases even closer than 30 Å) in the direction of the CNT extension.

IV. VAN DER WAALS INTERACTIONS AT INTERMEDIATE TO ASYMPTOTIC DISTANCES

From our ab initio vdW-DF calculations of the asymptotic van der Waals interactions we extract an analytical determination of the van der Waals interaction energy

E_{vdW} per unit length L for a nanotube pair as a function of the separation $d = 2R_{\text{geo}} + \Delta$. The analytical result for $E_{\text{vdW}}(d)/L$ rests on the approximation summarized in Refs. 40,41,50. It assumes that the electron densities of the two nanotubes do not overlap and constitute a lowest-order expansion⁵⁶ of Eq. (2) in terms of the *external-field* susceptibilities, α_{eff} :

$$E_{\text{vdW}} = - \int_0^\infty \frac{du}{2\pi} i \text{tr}[\alpha_{\text{eff},1} T_{12} \alpha_{\text{eff},2} T_{21}]. \quad (6)$$

Here T_{ij} denotes the dipole interaction tensor, $T_{ij} = -\nabla_i \nabla_j |\mathbf{r}_i - \mathbf{r}_j|^{-1}$. The analysis is possible to carry out for nonisotropic external-field susceptibilities,^{40,41} but for an interpretation of our vdW-DF calculations of CNT interactions it is sufficient to consider isotropic susceptibilities α_{eff} . We focus on the interaction regime where effects of the CNT morphology dominates the variation of $E_c^{\text{nl}} \approx E_{\text{vdW}}$ with distance.^{40,50} We assume a long-wavelength form of α_{eff} so that the resulting analytical determination remains valid at such intermediate-to-asymptotic interaction distances.

The physics of the local-field and external-field susceptibilities defines the parameterization of our vdW-DF method.^{20,22,23,43} The long-wavelength electrodynamic response determines the interaction at large distances⁴⁴ and our vdW-DF method describes this response by the isotropic effective (external-field) susceptibility²²

$$\alpha_{\text{eff}}^{\text{gg}}(u; \mathbf{r}) = \frac{n(\mathbf{r})}{u^2 + [9q_0^2(\mathbf{r})/(8\pi)]^2}. \quad (7)$$

We stress that our extraction of this long-wavelength form serves only to establish formal connection between the full vdW-DF calculations and the analytical approximation. We also emphasize that neither the effective response (7) nor the full vdW-DF response function²² is explicitly designed to accurately reproduce, for example, the static dielectric response, in contrast to the functional approaches described in Refs. 20,41,44 and 40. Rather, the full vdW-DF response function²² is constructed exclusively from an ansatz for the plasmon-pole response, conservation rules and many-body calculations^{22,53} to describe the average response. The full vdW-DF description involves contributions from different frequencies and wavelengths and it is the average response, rather than the long-wavelength limit (7), that determines the interactions at binding separations where our vdW-DF approach is most needed.

Our analysis focus on the intermediate-to-asymptotic separations furthermore allows us to consider the contributions to the susceptibility from the electron density averaged over the angular and along-tube variations. We thus substitute $\alpha_{\text{eff}}(\mathbf{r}; u) \rightarrow \bar{\alpha}_{\text{eff}}(s; u)$, where s denotes the radial distance from the nanotube center. The nanotube interaction per unit length, given in terms of the

effective response (7), becomes:⁴¹

$$\frac{E_{\text{vdW}}}{L} = - \int_0^\infty \frac{du}{2\pi} \int_0^\infty ds_1 s_1 \int_0^\infty ds_2 s_2 \bar{\alpha}_{\text{eff}}(s_1; u) \bar{\alpha}_{\text{eff}}(s_2; u) \sum_{\alpha, \beta = s, \theta, z} G_{\alpha, \beta}(s_1, s_2), \quad (8)$$

with the geometry factors

$$G_{\alpha\beta} = \int_0^{2\pi} d\theta_1 \int_0^{2\pi} d\theta_2 \int_0^\infty d(z_2 - z_1) [T_{12}^{\alpha\beta}(s_1, \theta_1, z_1; s_2, \theta_2, z_2)]^2, \quad (9)$$

where the dipole interaction tensors are expressed in cylindrical coordinates. The result (8) is easily expanded in the inverse center-of-mass separation d^{-1} of the nanotubes, yielding interaction energies of the form

$$\frac{E_{\text{vdW}}}{L} = -\frac{B_5}{d^5} - \frac{B_7}{d^7} + \dots, \quad (10)$$

with B_5 and B_7 given by

$$B_5 = \frac{9}{8} \int_0^\infty du \Xi^{(0)}(u)^2, \quad (11)$$

$$B_7 = \frac{225}{16} \int_0^\infty du \Xi^{(0)}(u) \Xi^{(2)}(u). \quad (12)$$

Here

$$\Xi^{(i)}(u) \equiv \int_0^\infty ds 2\pi s \bar{\alpha}_{\text{eff}}^{\text{gg}}(s; u) s^i, \quad (13)$$

is simply the i 'th moment of the effective response. We calculate the coefficients $B_{5,7}$ directly from the $\alpha_{\text{eff}}(s; u)$ variation specified by our underlying GGA-DFT calculations of the CNT electron density variation. We have explicitly tested consistency of this asymptotic evaluation and the set of full vdW-DF calculations for $\Delta > 16\text{--}20 \text{ \AA}$.

The relevant external-field electrodynamic response (α_{eff}) of the nanotubes is dominated by contributions at some radius $R > R_{\text{geo}}$. That is the experience gained from describing the electrodynamic response and van der Waals interactions of surfaces⁵⁷ and from previous investigation of the van der Waals bonding in graphitics.^{20,21} While the results presented in Refs. 40,41, 50 made the assumption that the response α_{eff} arose exclusively from the atom wall (at R_{geo}), the formal special-function evaluation^{41,58}

$$\frac{E_{\text{vdW}}(d, R)}{L} = -\frac{B_5}{d^5} {}_3F_2\left(\frac{1}{2}, \frac{5}{2}, \frac{5}{2}; 1, 1; \frac{4R^2}{d^2}\right), \quad (14)$$

is possible as long as we may assume the response α_{eff} dominated by contributions at any (single) radius R . The interaction result (14) simply reflects the morphology (interaction of two hollow cylinders). The effective vdW-DF response $\alpha_{\text{eff}}^{\text{gg}}(s; u)$ is dominated by contributions at R_{geo}

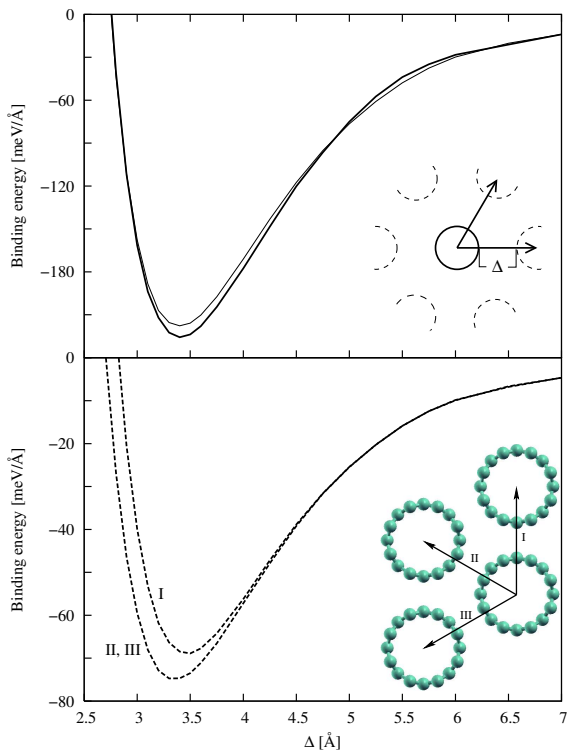


FIG. 3: Nanotube binding energy $E^{\text{vdW-DF}}(\Delta) - E^{\text{vdW-DF}}(\Delta \rightarrow \infty)$, (per unit length) for semiconducting (8,0) nanotubes evaluated in vdW-DF as a function of the wall-to-wall separation Δ . The top panel shows vdW-DF results for the hexagonal crystal and compares the crystal interaction energy (thick solid curve) against an estimate (thin solid curve) based on a sum of vdW-DF results for the nanotube pair interactions. The bottom panel reports vdW-DF calculations of the binding of two parallel nanotubes (dashed curves) in three different atomic configurations indicated in the insert. The sum of those three pair interactions constitutes the approximation for the crystal interaction (thin solid curve) in the top panel.

and outside in the CNT density tails. In this paper, we choose a value for the effective response radius

$$R_{\text{eff}} = \sqrt{\frac{2B_7}{25B_5}} \quad (15)$$

and obtain an analytical approximation

$$E_c^{\text{nl}}(\Delta) \approx E_{\text{vdW}}(d = 2R_{\text{geo}} + \Delta, R_{\text{eff}}). \quad (16)$$

that exactly reproduces the asymptotic variation of the full vdW-DF calculations up to the second spatial moment given by B_5 and B_7 . The relative position of R_{eff} and R_{geo} are shown in Fig. 2.

V. RESULTS AND DISCUSSION

A. van der Waals bonding in a nanotube crystal

The top panel of Fig. 3 reports our ab initio calculation (thick solid curve) of the vdW-DF binding in a hexagonal crystal of semiconducting (8,0) nanotubes. The vdW-DF result for the binding separation, $\Delta_{\text{bind}} \approx 3.45 \text{ \AA}$, is in very good agreement with experimental observations,^{4,5,6,7} $\Delta_{\text{exp}} \approx 3.4 \text{ \AA}$, and corrects the poor structure predicted in traditional LDA calculations²⁸ $\Delta_{\text{bind}}^{\text{LDA}} = 3.1 \text{ \AA}$. The binding energy for the nanotube bundle is large, $E_{\text{bind}}^{\text{crys}} = -30 \text{ meV/atom}$ corresponding to -0.225 eV/\AA , consistent with interaction strengths that we have previously calculated in vdW-DF for the interlayer binding in graphite:²¹ -50 meV/atom . The vdW-DF binding energy is significantly larger than the LDA result,²⁸ $\approx 10 \text{ meV/atom}$, obtained for a metallic (6,6) nanotube.

The figure documents differences between the vdW-DF calculation for the full CNT crystal (thick solid curve) and corresponding approximations based on CNT-pair contributions (thin solid curve). The regular vdW-DF calculations yield a CNT-crystal binding energy that is larger than the binding energy estimate obtained from the summation of pair contributions $E_{\text{bind}}^{\text{crys,est}} = -29 \text{ meV/atom}$ corresponding to -0.220 eV/\AA . We find that the vdW-DF energy difference $E_{\text{bind}}^{\text{crys}} - E_{\text{bind}}^{\text{crys,est}}$ is split evenly between contributions E_c^{nl} and E_0 .

Nevertheless, the vdW-DF results for the pair interaction energies constitute a fair approximation of the hexagonal ordering arising in the nanotube bundles. It is thus possible to use vdW-DF calculations of the CNT-pair interactions at general (parallel) configurations (of different relative rotations) to model the cohesion and binding in more general nanotube structures such as yarn and rope.

B. van der Waals bonding in a pair of parallel semiconducting nanotubes

Fig. 3, bottom panel, reports our ab initio calculation of the vdW bonding between pairs of parallel (8,0) nanotubes at three configurations ‘I’, ‘II’, and ‘III’, identified in the insert. These are the configurations that are relevant for the pair-interaction estimate of the CNT hexagonal crystal (thin solid curve in top panel). Even for a CNT pair, the nanotube binding is very significant, $E_{\text{bind}}^{\text{pair}} \approx -9.2 \text{ meV/atom}$, but occurs at slightly different binding separations for different relative nanotube rotations. We find that the vdW-DF results for the non-local correlation term E_c^{nl} are almost identical (smaller than 1% variation outside binding separations) for the three CNT-pair configurations. As is evident in the insert (which identifies actual atomic organization investigated in our vdW-DF method,) the atomic organization is in

better registry for some organization than others. There consequently exists some electron-density variation with the rotations and our vdW-DF method is sensitive to that variation since the semilocal contribution E_0 contains a description of the kinetic-energy repulsion.

As an interesting aside, we note that the high symmetry of the semiconducting (8,0) nanotube permits us to test the grid-sensitivity and consistency of the vdW-DF calculations. There must exist a four-fold symmetry in atomic positions around the (8,0) nanotube and such an approximate symmetry also emerges as a result of the initial atomic relaxation that we perform for an individual nanotube in traditional DFT. The symmetry implies a periodicity π in the variation of the vdW binding between a pair of nanotubes with the relative rotation angle Θ . However, the imperfect relaxation causes small variations in the exact atomic location relative to the grid. We find that the vdW-DF calculations are more sensitive than the underlying traditional DFT calculations. Nevertheless, the vdW-DF calculations respect the symmetry and produce vdW interaction energies for Θ and $\Theta + \pi$ relative rotations that are identical even at a sub-meV energy scale.

C. Approximative microscopic modeling for general nanotube-bundle structures

The comparison between the vdW-DF results for the nanotube crystal and for the approximation based on a sum of nanotube-pair interactions, Fig. 3, top panel, suggests a framework for an approximative microscopic modeling for the binding in more general bundles of (semiconducting) nanotubes. A simple mapping of the binding energy for two parallel nanotubes for all combinations of independent rotations (relative to the interaction line) provides the starting point. Adding such general pair-interaction contributions allows vdW-DF calculations to account for general vdW bonding in aligned nanotube structures, including nanotube yarn and ropes.

Moreover, the finding of insignificant differences between the E_c^{nl} energy contributions for the three nanotube-pair configurations investigated in Fig. 3, suggests an additional speed up in the modeling. Assuming that general, independent nanotube rotations also causes insignificant E_c^{nl} differences, it is sufficient to supplement one calculation of E_c^{nl} (detailed below) with a mapping of the general E^0 variation. This can be obtained at a computational cost equal to that of traditional implementations of DFT. A forthcoming study will provide vdW-DF results for the bundling of a broader set of semiconducting nanotubes and an explicit test of the $E^{\text{vdW-DF}}$ and E_c^{nl} variation with general (independent) nanotube-rotation angles to detail the suggested approximative modeling approach.

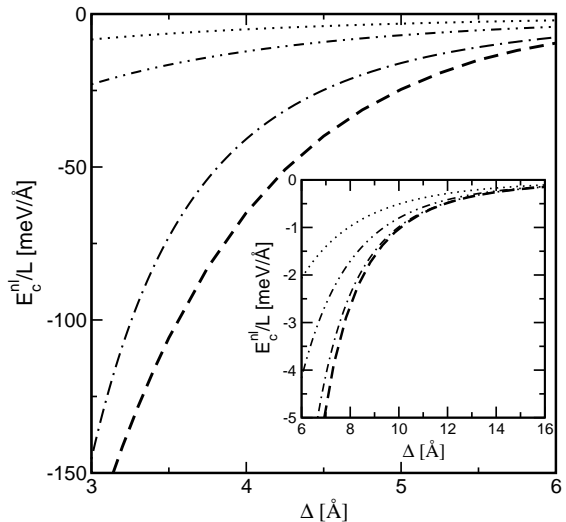


FIG. 4: Nonlocal correlation energy per unit length for a nanotube dimer near binding separations (main panel) and in the intermediate to asymptotic regime (insert panel). The thick dashed curves show the results of the full vdW-DF calculation of the nonlocal correlation energy (vdW interaction). The dotted and dashed-double-dotted curves show the (traditional) asymptotic interaction estimates as determined from the asymptotics $-B_5 d^{-5}$ and $-B_5 d^{-5} - B_7 d^{-7}$, respectively. Finally, the dashed-dotted curve shows the analytical evaluation that approximates the electrodynamical response by the long-wavelength form but retains a full description of the nanotube morphology. The analytical result also reflects the surface-physics insight that the electrodynamical response is dominated by contributions outside the radius defined by the atomic positions, Fig. 2.

D. Nature of the vdW bonding at bundle and at intermediate separations

Fig. 4 compares the full vdW-DF calculation of E_c^{nl} contribution to the CNT-pair interaction, thick dashed curves, with vdW-DF based approximations E_{vdW} , dotted and dash-dotted curves, near binding separations (main panel) and in the intermediate-to-asymptotic regime (insert). The contribution E_c^{nl} is evaluated for the configuration 'I' shown in the insert of the lower panel of Fig. 3 (but E_c^{nl} exhibits only insignificant differences between configurations 'I', 'II' and 'III'). All of the estimates E_{vdW} are, of course, independent of the nanotube rotation by construction. The dashed-dotted curves show the analytical CNT-pair interaction estimate (16) that invokes a long-wavelength form of the electrodynamic response but respects the morphology of the interaction problem.^{40,41} The dotted and dashed-double-dotted curves show (for $d = \Delta + 2R_{\text{geo}}$) traditional interaction estimates, $-B_5/d^5$ and $-B_5/d^5 - B_7/d^7$ respectively. The traditional interaction estimates clearly only become applicable in a very remote asymptotic regime beginning at $\Delta > 16$ Å.

The main panel shows that the full vdW-DF cal-

culations are necessary around the binding separations $\Delta_{\text{bind}} \sim 3.5 \text{ \AA}$. Here the interaction is significantly enhanced compared with estimates based on the asymptotic dipolar response. The enhancement is consistent with the behavior documented for graphite interactions as described in an earlier generation of vdW-DF.⁴³ The enhancement relative to the analytical approximations persists even beyond separations ($\Delta \approx 4 \text{ \AA}$) when there no longer exists an overlap of electron densities. It arises in part because the complete interaction also contains multipole interactions.²⁰

However, the contrast between the main panel and the insert panel in Fig. 4 also documents a qualitative change in nature in the mutual interaction with increasing separation. Gradually there is a transition in an intermediate-to-asymptotic regime (shown insert panel) where the mutual interaction is essentially specified by the morphology of the nanotube density variation as summarized in the analytical interactions estimate (16).

VI. CONCLUSIONS AND ACKNOWLEDGEMENT

We have presented ab initio calculations of the binding in nanotube bundles and in nanotube dimers. Our calculations rest on a density functional description²² that includes accounts of the dispersive forces. We have, in addition, presented an analytical evaluation valid at intermediate to large nanotube separation.

Our microscopic theory of the CNT binding of semi-conducting (8,0) CNTs provides a number of results based on the ab initio vdW-DF calculations. The CNT study supplements recent microscopic theory studies of elements of the DNA base-pair interaction²⁶ and of the polyethylene polymer crystal²⁴ in a broader goal of developing a microscopic theory of self-organization and

bundling of nanoscale filaments. This vdW-DF study finds a nanotube wall-to-wall separation in very good agreement with experiments and predicts a vdW bonding with a significant strength, consistent with recent measurements for graphitics.²⁹

Our work furthermore constitutes an analysis that details the nature of the mutual CNT interactions by identifying a set of distinct interaction regimes. We provide an analytical approximation for the CNT pair interactions at distances when the electron densities are nonoverlapping and the dielectric response are dominated by the long-wavelength form. Comparing against our ab initio vdW-DF calculations (valid at general distances) we thereby identify a relatively broad intermediate-to-asymptotic regime where the interaction form is primarily defined by the CNT morphology.

Finally, this introductory study also suggests a framework for an efficient implementation of quantum-physical modeling of the CNT bundling in more general geometries, including nanotube yarn and ropes. The vdW-DF study documents that a summation of nanotube-pair interaction energies represents a fair approximation for the nanotube-crystal binding energy when the CNT-pair interaction is calculated in vdW-DF. A simple vdW-DF mapping of the nanotube-pair interaction for general (independent) CNT rotations relative to the interaction axis therefore provides adequate input for describing the vdW bonding in general aligned CNT structures.

We thank B. I. Lundqvist for useful discussions and L. Glasser for suggesting and detailing the special-function evaluation (14) from our corresponding parallel-nanotube interaction result in Ref. 50. Support from the Swedish Research Council, the Swedish Foundation for Strategic Research, the Swedish National Graduate School in Materials Science, as well as allocation of computer time at SNIC (Swedish National Infrastructure for Computing) is gratefully acknowledged.

* Electronic address: hylgdaar@chalmers.se

¹ M. S. Dresselhaus, G. Dresselhaus, and Ph. Avouris, *Carbon Nanotubes, Synthesis, Structure, Properties, and Applications* (Springer Verlag, Berlin-Heidelberg New York, 2001).

² M. M. Treacy, T. Ebbesen, and J. M. Gibson, *Nature* **381**, 678 (1996); J. P. Lu, *Phys. Rev. Lett.* **79**, 1297 (1997).

³ R. R. Schlittler, J. W. Seo, J. K. Gimzewski, C. Durkan, M. S. Saifullah, and M. E. Welland, *Science* **292**, 1136 (2001).

⁴ S. Iijima, *Nature* **354**, 56 (1991).

⁵ X. F. Zhang, X. B. Zhang, G. Van Tendeloo, S. Amelinckx, M. Op de Beeck, and J. Van Landuyt, *J. Cryst. Growth* **130**, 368 (1993).

⁶ M. Terrones, N. Grobert, J. Olivares, J. P. Zhang, H. Terrones, K. Kordatos, W. K. Hsu, J. P. Hare, P. D. Townsend, K. Prassides, A. K. Cheetham, H. W. Kroto, D. R. M. Walton, *Nature* **388**, 52 (1997).

⁷ C.-H. Kiang, M. Endo, P. M. Ajayan, G. Dresselhaus,

M. S. Dresselhaus, *Phys. Rev. Lett.* **81**, 1869 (1998).

⁸ Y.-L. Li, I. Kinloch, and A.H. Windle, *Science* **304**, 276 (2004).

⁹ M. Zhang, K.R. Atkinson, and R.H. Baughman, *Science* **306**, 1358 (2004).

¹⁰ L.M. Ericson *et al.*, *Science* **305**, 1447 (2004).

¹¹ J. Hwang, *et al.*, *Phys. Rev. B* **62**, R13310 (2000).

¹² X. Blase, L. X. Benedict, E. L. Shirley, and S. G. Louie, *Phys. Rev. Lett.* **72**, 1878 (1994); D. Sánchez-Portal, E. Artacho, and J. M. Soler, A. Rubio, and P. Ordejón, *Phys. Rev. B* **59**, 12678 (1999).

¹³ See, for example, V. Barone and G. E. Scuseria *J. Chem. Phys.* **121**, 10376 (2004).

¹⁴ For example in the parametrization J. P. Perdew and A. Zunger, *Phys. Rev. B* **23**, 5048 (1981).

¹⁵ J.P. Perdew, K. Burke, and M. Ernzerhof, *Phys. Rev. Lett.* **77**, 3865 (1996).

¹⁶ A. Kis, G. Csányi, J.-P. Salvetat, T.-N. Lee, E. Couteau, A. J. Kulik, W. Benoit, J. Brugger, and L. Ferró, *Nature*

- materials **3**, 153 (2004).
- ¹⁷ For a description of corresponding LDA problems in providing a transferable description for polymer crystals, please see M. S. Miao *et al.*, *J. Chem. Phys.* **115**, 11317 (2001).
- ¹⁸ J. M. Pérez-Jordá and A. D. Becke, *Chem. Phys. Lett.* **233**, 134 (1995).
- ¹⁹ H. Rydberg, N. Jacobson, P. Hyldgaard, S.I. Simak, B.I. Lundqvist, and D.C. Langreth, *Surf. Sci.* **532-535**, 606 (2003).
- ²⁰ H. Rydberg, M. Dion, N. Jacobson, E. Schröder, P. Hyldgaard, S.I. Simak, D.C. Langreth, and B.I. Lundqvist, *Phys. Rev. Lett.* **91**, 126402 (2003).
- ²¹ E. Ziambaras, J. Kleis, E. Schröder, and P. Hyldgaard, *Phys. Rev. B* **76**, 155425 (2007).
- ²² M. Dion, H. Rydberg, E. Schröder, D.C. Langreth, and B.I. Lundqvist, *Phys. Rev. Lett.* **92**, 246401 (2004); **95** 109902(E) (2005).
- ²³ T. Thonhauser, V. R. Cooper, S. Li, A. Puzder, P. Hyldgaard and D.C. Langreth, *Phys. Rev. B* **76**, 125112 (2007).
- ²⁴ J. Kleis, B.I. Lundqvist, D.C. Langreth, and E. Schröder, *Phys. Rev. B* **76**, 100201(R) (2007).
- ²⁵ See, for example, G. Avitabile *et al.*, *J. Polym. Sci. Lett. Ed.* **13**, 351 (1975).
- ²⁶ V.R. Cooper, T. Thonhauser, A. Puzder, E. Schröder, B. I. Lundqvist, and D.C. Langreth, *J. Am. Chem. Soc.* **130**, 1304 (2008); A. Puzder, M. Dion, and D. C. Langreth, *J. Chem. Phys.* **124**, 164105 (2006); T. Thonhauser, A. Puzder, and D. C. Langreth, *J. Chem. Phys.* **124**, 164106 (2006).
- ²⁷ A quick set of DFT-GGA calculations produce an extremely shallow binding-indication at much too large distances and representing only 5% of the presently report vdW-DF binding.
- ²⁸ J.-C. Charlier, X. Gonze, and J.-P. Michenaud, *Europhys. Lett.* **29**, 43 (1995); S. Reich, C. Thomsen, P. Ordejón, *Phys. Rev. B* **65**, 155411 (2002).
- ²⁹ R. Zacharia, H. Ulbricht, and T. Hertel, *Phys. Rev. B* **69**, 155406 (2004).
- ³⁰ J. Q. Sun and R. J. Bartlett, *J. Chem. Phys.* **104**, 8553 (1996); S. Hirata and S. Iwata, *J. Chem. Phys.* **109**, 4147 (1998); S. Suhai, *Phys. Rev. B* **27**, 3506 (1983).
- ³¹ P. Y. Ayala and G. E. Scuseria, *J. Chem. Phys.* **110**, 3660 (1999).
- ³² P. Y. Ayala, K. N. Kudin, and G. E. Scuseria, *J. Chem. Phys.* **115**, 9698 (2001).
- ³³ S. D. Chakarova-Käck, E. Schröder, B.I. Lundqvist and D.C. Langreth, *Phys. Rev. Lett.* **96**, 146107 (2006).
- ³⁴ S. D. Chakarova-Käck, Ø. Borck, E. Schröder, and B. I. Lundqvist, *Phys. Rev. B* **74**, 155402 (2006).
- ³⁵ A parallel project investigates the adhesion of graphite on SiC in a surface unit-cell that have the graphite-sheet overlayer relaxed to 2% strain; E. Ziambaras, C. Ruberto, B.I. Lundqvist, and P. Hyldgaard, unpublished.
- ³⁶ Y. U. Barash and O. I. Notysh, *Zh. Eksp. Fyz.* **98**, 542 (1990).
- ³⁷ B. E. Sernelius and P. Björk, *Phys. Rev. B* **57**, 6592 (1998).
- ³⁸ M. Boström and B. E. Sernelius, *Phys. Rev. B* **61**, 2204 (2000).
- ³⁹ J. F. Dobson, A. White, and A. Rubio, *Phys. Rev. Lett.* **96**, 073201 (2006).
- ⁴⁰ E. Schröder and P. Hyldgaard, *Surf. Sci.* **532**, 880 (2003).
- ⁴¹ J. Kleis, P. Hyldgaard, and E. Schröder, *Comp. Mat. Sci.* **33**, 192 (2005).
- ⁴² DACAPO from <http://wiki.fysik.dtu.dk/dacapo/>.
- ⁴³ H. Rydberg, B. I. Lundqvist, D. C. Langreth, and M. Dion, *Phys. Rev. B* **62**, 6997 (2000).
- ⁴⁴ D.C. Langreth, M. Dion, H. Rydberg, E. Schröder, P. Hyldgaard, and B.I. Lundqvist, *Int. J. Quant. Chem.* **101**, 599 (2005).
- ⁴⁵ W. Kohn, Y. Meir, D. E. Makarov, *Phys. Rev. Lett.* **80**, 4153 (1998).
- ⁴⁶ S. Kurth and J. P. Perdew, *Phys. Rev. B* **59**, 10461 (1999).
- ⁴⁷ J. F. Dobson and J. Wang, *Phys. Rev. Lett.* **82**, 2123 (1999); *Phys. Rev. B* **62**, 10038 (2000); J. F. Dobson and B. P. Dinte, *Phys. Rev. Lett.* **76**, 1780 (1996).
- ⁴⁸ J. M. Pitarke and J. P. Perdew, *Phys. Rev. B* **67**, 045101 (2003).
- ⁴⁹ For illustrations of applications to model, molecular, and/or solid systems, see, for example, J. Jung, P. Garcia-Gonzalez, J. F. Dobson, and R. W. Godby, *Phys. Rev. B* **70**, 205107 (2004); F. Furche and T. Voorhis, *J. Chem. Phys.* **122**, 164106 (2005); M. Fuchs and X. Gonze, *Phys. Rev. B* **65**, 235109 (2002); M. Fuchs, K. Burke, Y.-M. Niquet, and X. Gonze, *Phys. Rev. Lett.* **90**, 189701 (2003); F. Aryasetiawan, T. Miyake, and K. Terakura, *Phys. Rev. Lett.* **88**, 166401 (2002); T. Miyake, F. Aryasetiawan, T. Kotani, M. van Schilfhaarde, M. Usuda, and K. Terakura, *Phys. Rev. B* **66**, 245103 (2002); A. Marini, P. Garcia-Gonzalez, and A. Rubio, *Phys. Rev. Lett.* **96**, 136404 (2006).
- ⁵⁰ E. Schröder and P. Hyldgaard, *Mat. Sci. Eng. C* **23**, 721 (2003).
- ⁵¹ C. Amovilli and N. H. March, *Carbon* **43**, 1624 (2005).
- ⁵² H.J. Monkhorst and J.D. Pack, *Phys. Rev. B* **13**, 5188 (1976).
- ⁵³ D.C. Langreth and S.H. Vosko, *Adv. Quantum Chem.* **21**, 175 (1990).
- ⁵⁴ Y. Zhang and W. Yang, *Phys. Rev. Lett.* **80**, 890 (1998).
- ⁵⁵ X. Wu, M.C. Vargas, S. Nayak, V. Lotrich, and G. Scoles, *J. Chem. Phys.* **115**, 8748 (2001).
- ⁵⁶ B. I. Lundqvist, Y. Andersson, H. Shao, S. Chan, D. C. Langreth, *Int. J. Quant. Chem.* **56**, 247 (1995).
- ⁵⁷ See, for example, E. Zaremba and W. Kohn, *Phys. Rev. B* **13**, 2270 (1976); B. N. J. Persson and P. Apell, *Phys. Rev. B* **27**, 6058 (1983); B. N. J. Persson and E. Zaremba, *Phys. Rev. B* **30**, 5669 (1984); A. Liebsch, *Phys. Rev. B* **33**, 7249 (1986); E. Hult, H. Rydberg, B.I. Lundqvist, and D.C. Langreth, *Phys. Rev. B* **59**, 4708 (1999); E. Hult, P. Hyldgaard, J. Rossmeisl, and B.I. Lundqvist, *Phys. Rev. B* **64**, 195414 (2001).
- ⁵⁸ L. Glasser, Clarkson University, private communication.